Thermoelectric power of cerium and ytterbium intermetallics

V. Zlatić* and B. Horvatić
Institute of Physics, Bijenička cesta 46, P.O. Box 304, HR-10001 Zagreb, Croatia

I. Milat
Institute for Theoretical Physics, ETH-Hönggerberg, CH-8093 Zürich, Switzerland

B. Coqblin
Laboratoire de Physique des Solides, Université Paris-Sud, Bâtiment 510, 91405-Orsay, France

G. Czycholl and C. Grenzebach
Institute for Theoretical Physics, Bremen University, D-28334 Bremen, Germany
(Received 7 April 2003; revised manuscript received 8 July 2003; published 29 September 2003)

The temperature dependence of the thermoelectric power (TEP) of metallic systems with cerium and ytterbium ions exhibits characteristic features which we explain by the Coqblin-Schrieffer model (CSM). We specify a given system by the degeneracy and splitting of the crystal-field (CF) levels, the strength of the exchange and potential scattering, and the number of f electrons or f holes; for cerium and ytterbium ions we assume $n_f \leqslant 1$ and $n_f^{hole} \leqslant 1$, respectively. The Kondo temperature T_K is then generated by the ''poor man's scaling''; it separates a local-moment (LM) from a Fermi-liquid (FL) regime. In the LM regime ($T \geqslant T_K$) we calculate the TEP by a renormalized perturbation expansion, in which the exchange coupling J is also renormalized by the poor man's scaling. This gives the TEP with a large peak at high temperatures and a sign change at $T_x \simeq \alpha T_K$, where for parameters used in this paper we have α between roughly 2.5 and 10. For $n_f \simeq 1$ and large CF splitting, we find a broad temperature range $T_K \ll T \leqslant T_x$, in which the TEP of the CSM is negative. In the FL regime ($T \leqslant T_K$) we neglect the excited CF states, reduce the CSM to an effective spin-degenerate exchange model, map it on an effective spin-degenerate Anderson model, and calculate the TEP by an expansion in terms of $U \propto 1/J$. For cerium ions ($n_f \leqslant 1$) we obtain in this way the TEP which follows for $T \ll T_K$ a linear FL law, attains at about $T_K/2$ a positive maximum, and changes sign above T_K. The results pertaining to ytterbium ions ($n_f^{hole} \leqslant 1$) are obtained by reflecting the $n_f \leqslant 1$ curves on the temperature axis. The overall results obtained for the CSM in such a way explain the essential features of the temperature, pressure, and doping dependence of the TEP in cerium and ytterbium systems. Unfortunately, neither our high-temperature nor the low-temperature expansion provide the details or locate the minimum of the negative TEP which we find in the transition region between the FL and LM regimes.

DOI: 10.1103/PhysRevB.68.104432 PACS number(s): 71.27.+a, 71.28.+d, 72.15.Qm, 72.15.Jf

I. INTRODUCTION

The thermoelectric properties of intermetallic compounds with Ce and Yb ions with one f electron or f hole show many interesting features[1–47] which are not found in normal metals or semiconductors. At sufficiently high temperatures the thermoelectric power (TEP) has very often a positive peak in cerium systems and a negative one in ytterbium systems. In a number of cases, the TEP assumes giant values and much of recent interest in heavy-fermion thermoelectricity is due to the belief that some of the new systems, with the thermopower larger than 150 μV/K, might be useful for application in the liquid nitrogen range.[48] At low temperatures the TEP can be quite complicated and, considered as a function of temperature, $S(T)$, it often exhibits a nonmonotonic behavior and a sign change. However, systems with similar thermopowers exhibit similarities in other thermodynamic and transport properties as well, and the shape of $S(T)$ can be used to classify Ce and Yb intermetallics and alloys into well-defined groups.[35,36]

The anomalous thermoelectric properties of Ce and Yb intermetallics have stimulated a lot of theoretical work, but the interpretation of the experimental data is still controversial.[49–60] Here, we show that the experimental results can be qualitatively understood in terms of the Coqblin-Schrieffer model[61] (CSM) which describes the dynamics of conduction electrons due to the exchange and potential scattering on incoherent $4f^1$ states of Ce or the $4f^{13}$ states of Yb. We take into account the splitting of the f states due to the crystalline electric field (CF) but consider only the simplest case of two CF levels with the energy separation Δ and the degeneracy of the ground and excited CF levels given by m and M, respectively. The number of f electrons or f holes is restricted to $n_f \leqslant 1$ for Ce ions and to $n_f^{hole} \leqslant 1$ for Yb ions. The CSM seems to capture the main features of the thermoelectric power data of most Ce- and Yb-based systems, even though the coherent scattering of conduction electrons on the f ions is neglected and the loss of electrical resistance in stoichiometric compounds at low temperatures is not accounted for. Using the ''poor man's scaling''[62–66] it is easy to show that the CSM is characterized by the Kondo temperature T_K, such that for $T > T_K$ the system is in the weak-coupling, local-moment (LM) regime and for $T < T_K$ it is in the strong-coupling regime. The scaling also shows[64,65] that

the CF splitting greatly reduces T_K with respect to the Kondo temperature of an $(m+M)$-fold degenerate CSM, T_K^H.

The CSM is an approximation to a more general single-impurity Anderson model (SIAM), from which it is derived by the Schrieffer-Wolff (SW) transformation.[63,67] This eliminates the hybridization between the conduction states and the f states, and generates the exchange and potential scattering of the CSM. The low-energy excitations and the transport and thermodynamic properties of both models should be the same. In order to keep $n_f \leqslant 1$ and $n_f^{hole} \leqslant 1$, as required for Ce and Yb systems, respectively, the on-site Coulomb correlation of the SIAM should be very large. Furthermore, the SIAM with less than one f electron (or less than one f hole) distributed over $m+M$ states is far away from the electron-hole symmetry. Thus, the SW transformation generates the CSM with an antiferromagnetic exchange coupling and a potential scattering term which is negative for Ce and positive for Yb ions.[66] Since the asymmetry of the underlying SIAM increases as the system moves further away from the electron-hole symmetry, the magnitudes of both the exchange and potential scattering terms increase as n_f (or n_f^{hole}) decrease from 1. These considerations allow us to treat the effects of pressure or chemical pressure on the TEP of Ce and Yb systems by the CSM.

At high temperatures $T > T_K$, the TEP is calculated by the third-order renormalized perturbation expansion[69] (RPT), in which the exchange coupling J is renormalized by the poor man's scaling. At low temperatures $T \leqslant T_K$, the CSM has a crossover to the strong-coupling regime and direct thermopower calculations become quite difficult. However, the simplifications arise close to the ground state, which is known to be a Fermi liquid (FL).[66,68] For large CF splitting and $k_B T \leqslant k_B T_K \ll \Delta$, the excited CF states of the CSM can be neglected and the ensuing m-fold degenerate Kondo model becomes equivalent to an m-fold degenerate SIAM with SU(m) symmetry and large on-site Coulomb repulsion $U \propto 1/J$ between f electrons of the opposite spin.[67] The strong-coupling features of the CSM and SIAM are the same, provided we choose the parameters in such a way that the Kondo scale of both models is the same. The FL properties are then obtained by the modified perturbation theory[70] (MPT) which interpolates between the weak-coupling result[71–73] and the exact atomic limit of the SIAM.

Using these perturbation expansions, the high-temperature one in terms of J and the low-temperature one in terms of U, we find the TEP which can have pronounced peaks at high and low temperatures due to an interplay between the Kondo effect and CF splitting. We also find that the TEP can become negative at the crossover between the LM and FL regimes, but our calculations cannot provide the actual shape of $S(T)$ in the transition region, and the overall behavior of the TEP can only be inferred from an interpolation between the low- and high-temperature results.

The paper is organized as follows. First we describe the experimental data. Then we discuss the high-temperature TEP of the CSM obtained by the RPT and the low-temperature TEP of the SIAM obtained by the MPT. Finally, we use our results to discuss the experimental data.

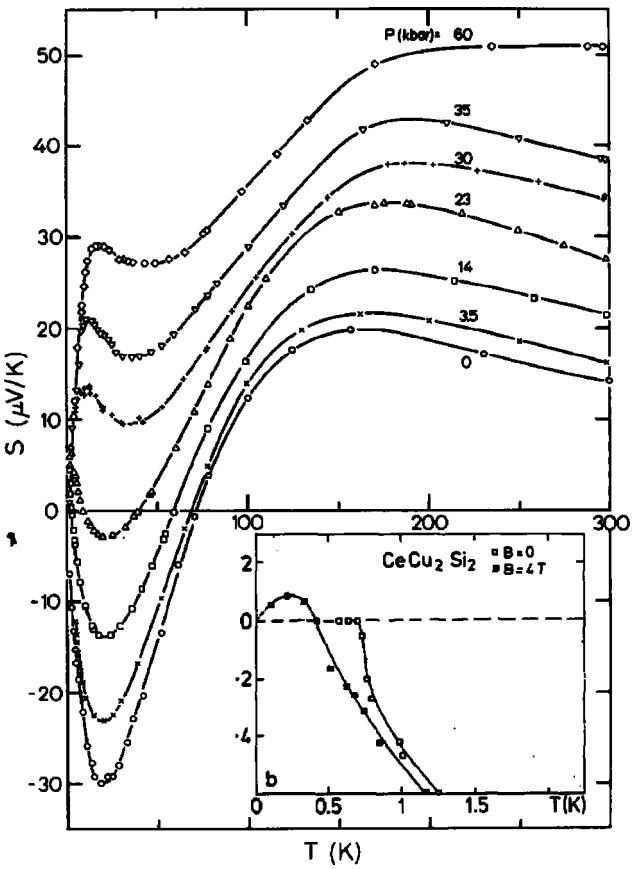

FIG. 1. The thermopower of $CeCu_2Si_2$ plotted as a function of temperature for various pressures (Ref. 13). The inset shows the low-temperature data (Ref. 8) at ambient pressure and small magnetic field, which suppresses the superconducting transition and reveals the positive TEP peak. Type (a) behavior is seen at zero pressure, type (b) between 14 kbar and 23 kbar, and type (c) at 30 kbar and above.

II. DESCRIPTION OF THE EXPERIMENTAL DATA

The experimental results of cerium and ytterbium intermetallics exhibit some characteristic features which separate them into distinct groups.[35,36] First of all, the TEP curves of Kondo compounds with Ce ions have a large positive peak at a sufficiently high temperature, which corresponds to a fraction of the CF splitting. The low-temperature behavior of Ce Kondo systems is more complicated, and one often finds a negative minimum and an additional positive peak at still lower temperatures. Typical shapes are illustrated by Fig. 1, where the TEP of $CeCu_2Si_2$,[13] measured at various pressures, is shown as a function of temperature. The TEP curves of Yb systems exhibit at high temperatures a large negative peak, which mirrors the Ce curves, as one would expect in a system with f holes. In what follows we provide a more detailed description of the TEP due to the Ce and Yb Kondo ions.

The first type of thermopower curve [type (a)] is characterized by a broad positive high-temperature peak between 100 K and 200 K and by a deep negative minimum at lower temperatures. TEP like that is observed in Ce_xLa_{1-x},[4] $CeCu_2Si_2$,[6,8,13] $CeCu_2Ge_2$,[15,32,36] $CePd_2Si_2$,[12,36] CePdAl,[47]

$CePdIn$,[25] $CePtSn$,[25] $CePb_3$,[15] $Ce(Pb_{1-x}Sn_x)_3$,[23] $CeRh_{2-x}Ni_xSi_2$ for small x,[24] and $CeNi_2Sn_2$.[35] Most of these systems order magnetically or become superconducting at lowest temperatures.

The second type (b) for the thermopower is similar to type (a), except that at very low temperatures the thermopower changes sign again and exhibits an additional positive peak. A typical example is provided by $CeAl_3$.[1,8,14] The first experimental results[1] gave a pronounced positive maximum at roughly 60 K, which was accounted for by the CSM with CF effects.[50] Then, more recent experiments[8,14] gave a change of sign at roughly 8 K, a weak negative minimum at roughly 4 K, another change of sign at roughly 0.4 K, and a small positive maximum at roughly 0.1 K. These features cannot be explained by the unrenormalized third-order perturbation expansion of the CSM,[50] but do follow from the calculations presented here. The type (b) for the TEP is found in several dilute Ce alloys, like $Ce_xLa_{1-x}Al_3$,[1,31] $Ce_xLa_{1-x}Ni$,[18] and $Ce_xLa_{1-x}Pd_2Si_2$,[33] in stoichiometric compounds, like $CeAl_3$, $CePdSn$,[25,35,43] $CePdGe$, and $CePtGe$,[44] as well as in some concentrated Ce alloys, like $Ce_xLa_{1-x}Cu_2Si_2$.[7] In some cases the positive low-temperature peak is canceled by superconducting or magnetic transitions. For example, in $CeCu_2Si_2$,[8] the positive low-temperature upturn is seen only in an external magnetic field which suppresses the superconducting transition. Experimental evidence is now accumulating that the slope $S(T)/T$ is indeed positive in most Ce heavy fermions if the measurements are performed at low enough temperature and with sufficient accuracy.[43,44,47]

Finally, the third type (c) describes the TEP which is always positive but has a small peak at low temperatures and a large one at high temperatures. The TEP does not change its sign between these two peaks, as it does in type (b) systems. This behavior is observed in many cerium Kondo systems, like $Ce_x(La_{1-z}Y_z)_{1-x}Al_2$,[3] $Ce_xLa_{1-x}Cu_6$ for small x,[17] and $Ce_xLa_{1-x}Ru_2Si_2$,[19] in Ce-rich compounds like $Ce(Pb_{1-z}Sn_z)$,[23] $CeRu_2Si_2$,[20] and $Ce(Cu_xAu_{1-z})_6$ for small x,[26] and also in $Ce_xLa_{1-x}Ni_{0.8}Pt_{0.2}$,[34] $Ce_xLa_{1-x}Cu_2Si_2$,[37,45] and $Ce_xY_{1-x}Cu_2Si_2$.[46] In some cases, the high-temperature peak is very broad and only a shoulder remains on its low-temperature side, as in $Ce(In_{1-x}Sn_x)_3$ and $Ce_{1-x}La_xIn_3$ for small x,[10] $CeCu_6$ and $Ce_xLa_{1-x}Cu_6$ for large x,[17] $CeInCu_2$,[28] $CeCu_3Ga_2$, $CeCu_3Al_2$,[30] $CeNiIn$ and $CePtIn$,[25] and $CeNiGe$.[44] We classify a behavior like that as type (d).

The high-pressure studies of the TEP of cerium compounds also reveal some typical features, which are shown in Fig. 1 for the case of $CeCu_2Si_2$.[13] Similar effects are found in other compounds, like $CeCu_2Ge_2$,[32,36] $CePd_2Si_2$,[36] or $CeAl_3$.[21] Pressure reduces the large negative low-temperature peak and gives rise to a positive peak at lowest temperatures. This low-temperature peak is separated from the large positive high-temperature peak by a temperature interval in which the TEP is first negative (for smaller pressure) and then positive (for higher pressure). Finally, at very high pressure (not shown in Fig. 1) only a positive high-temperature peak with a more or less pronounced shoulder remains. Thus, the TEP transforms under pressure from type (a) to type (b) and finally to type (c) or (d).

Doping affects the shape of the TEP in a similar way as pressure. An increase of Ce concentration, leading to the reduction of the lattice constant, transforms the $S(T)$ of $Ce_xLa_{1-x}Pd_2Si_2$ (Ref. 33) from type (a) to type (b). In dilute $Ce_xLa_{1-x}Cu_{2.05}Si_2$ (Ref. 45) an increase of Ce enhances the low-temperature peak and brings it closer to the huge high-temperature peak. In $Ce_xLa_{1-x}Cu_6$ (Ref. 17) one finds for $x<0.5$ two peaks separated by a well-resolved minimum, while for $x>0.9$ only a single hump with a shoulder on the low-temperature side remains.[34] In $Ce(Cu_xAl_{1-x})_2$ and $Ce(Ni_xAl_{1-x})_2$ (Ref. 22) the copper or nickel substitution reduces the lattice constant, and we observe $S(T)$ changing from type (a) to type (c) as x is increased from zero up to 20%. Similarly, $Ce(Pb_{1-x}Sn_x)_3$ (Ref. 23) changes from type (a) to type (c) as x is increased. On the other hand, replacing Y ions by larger Ce ions in dilute $Ce_xY_{1-x}Cu_2Si_2$ (Ref. 46) expands the lattice and transforms $S(T)$ from a single-peak [type (d)] to a two-peak structure [type (c)]. A behavior like that is consistent with the ''chemical pressure effects,'' although doping might involve a charge transfer or change the character of the ground state and is more complex than just the hydrostatic pressure.[74]

Next, we discuss briefly the case of the ytterbium intermetallics, which exhibit, generally, a large negative TEP peak at high temperatures. A thermopower with a single peak is found in systems like $YbAl_3$,[2] $YbAgCu_4$,[27] Yb_2Cu_7,[30] or $YbCu_2Si_2$,[42] which mirrors the type (d) behavior of Ce systems. The nonmonotonic low-temperature behavior is found in Yb systems as well. A TEP with a large negative peak, followed by a positive peak at lower temperatures and in some cases by an additional negative peak at lowest temperatures, is found in $YbSi$,[42] $Yb(Ni_xCu_{1-x})_2Si_2$ for large x,[39] $YbAu_2$ and $YbAu_3$,[38] $YbPtIn$,[41] and $Yb_2Rh_3Al_9$.[40] A behavior like that mirrors the type (a) and (b) behavior of Ce systems. The nonmonotonic low-temperature behavior without a sign change is found in $Yb_2Ir_3Al_9$,[40] $YbPdCu_4$,[27] or $Yb(Ni_xCu_{1-x})_2Si_2$ for small x,[39] which mirrors the type (c) behavior of Ce systems. As regards the effects of pressure and doping in Yb systems, the reduction of atomic volume stabilizes the magnetic $4f^{13}$ configuration and reduces the Kondo temperature. Thus, it is not surprising that applying pressure to $YbSi$ (Ref. 42) or substituting Cu for Ni in $Yb(Ni_xCu_{1-x})_2Si_2$ (Ref. 39) (positive chemical pressure) produces similar effects as negative pressure or La doping in $CeCu_6$.

In summary, the experimental data show that, regardless of the concentration of magnetic ions, the TEP of Ce and Yb intermetallics assumes a few characteristic shapes. The peaks in the thermoelectric power of dilute alloys correlate, in general, with the logarithms in the electrical resistance[45,46] and with the transition between various magnetic regimes that one sees in the magnetic susceptibility data.[75,76] We take that as an indication that the TEP is due to the exchange scattering of conduction electrons on the $4f$ states of Ce or Yb ions and show that the temperature, pressure, and doping dependence of the data can be accounted for by the CSM.

III. HIGH-TEMPERATURE THEORETICAL MODEL

The high-temperature properties of metallic systems with rare-earth ions are described by the Coqblin-Schrieffer

Hamiltonian[61] with the CF splitting,[69]

$$H_{CS}=\sum_{\nu} E_{\nu}a_{\nu}^{\dagger}a_{\nu}+\sum_{\mathbf{k}}\sum_{\nu}\epsilon_{\mathbf{k}}c_{\mathbf{k}\nu}^{\dagger}c_{\mathbf{k}\nu}$$
$$-J_0\sum_{\mathbf{k},\mathbf{k}'}\sum_{\nu,\nu'}c_{\mathbf{k}'\nu'}^{\dagger}c_{\mathbf{k}\nu}(a_{\nu}^{\dagger}a_{\nu'}-\delta_{\nu,\nu'}\langle n_{\nu}\rangle)$$
$$+\sum_{\mathbf{k},\mathbf{k}'}\sum_{\nu}(V_0-J_0\langle n_{\nu}\rangle)c_{\mathbf{k}'\nu}^{\dagger}c_{\mathbf{k}\nu}, \qquad (1)$$

where all the symbols have their usual meaning.[69] The first term describes the CF-split $4f^1$ state of Ce ions or $4f^{13}$ state of Yb ions, the second term describes the conduction band of width $2D_0$ and a constant density of states $\rho_0=1/(2D_0)$, the third term defines the pure (nondiagonal) exchange scattering between $4f^1$ states and band electrons, and the last term is the total (diagonal) potential scattering. The summation over ν is over all the CF states, and J_0 and V_0 are the coupling constants, which are assumed to be ν independent. For simplicity, we represent the $4f^1$ electron of Ce (the $4f^{13}$ hole of Yb) by the lowest $J=\frac{5}{2}$ ($J=\frac{7}{2}$) spin-orbit state and consider a cubic CF splitting with the ground-state level at E_m and an excited state at E_M. The energy separation between the ground and excited states is $E_M-E_m=\Delta$, and they are *m*-fold and *M*-fold degenerate, respectively. The electron number operators commute with H_{CS}, because the model neglects the quantum mixing of ionic configurations with different numbers of electrons; i.e., the average value of n_f cannot be changed except by thermal fluctuations. The CSM provides an accurate description of random magnetic impurities and is most appropriate for dilute alloys. It also applies to concentrated Ce and Yb systems at temperatures such that the scattering of conduction electrons on the rare-earth ions is incoherent. Surprisingly, the CSM seems also to account for the low-temperature TEP of stoichiometric compounds.

The high-temperature heat and charge transport is described by the Boltzmann equation and the scattering rate for the transport relaxation time is evaluated up to the third order in the scattering potential.[50,55,69] All the computational details can be found in the papers by Cornut and Coqblin[69] and Bhattacharjee and Coqblin[50] (BC). These calculations are expected to be reliable in the LM regime, and the qualitative features of the thermopower obtained in this way can be summarized as follows. For $k_BT>\Delta$, the thermopower is small and behaves as $1/T$. As temperature decreases, the thermopower increases up to a large (positive or negative) value at about $k_BT_{max}\simeq\Delta/3$. The sign and slope of S depend on the relative size of J_0 and V_0, and for the parameters in the physical range one easily finds the peak value of thermopower above 50 μV/K. Thus, the BC theory captures the essential high-temperature features of Ce and Yb intermetallics. However, for $k_BT\ll\Delta$, the TEP decreases monotonically towards the zero-temperature value, which shows that the unrenormalized third-order perturbation theory becomes unreliable at rather high temperatures and cannot describe the change of sign of the TEP below T_{max}. The perturbation expansion can be extended to lower temperatures by including the higher-order diagrams or by summing the whole classes of diagrams and renormalizing the coupling constants. Here we use the RPT in which the exchange coupling J is renormalized by the poor man's scaling.[62–66]

The scaling equations of the CSM are generated by reducing the conduction-electron cutoff in Eq. (1) from D_0 to D and simultaneously rescaling the coupling constant for the spin-flip scattering, $J(D)$, so as to keep the low-energy excitations of the total system unchanged.[62] The solution, valid up to the second order in renormalized couplings, reads[64]

$$\exp\left(\frac{1}{\rho_0 J}\right)=\left(\frac{k_BT_K}{D}\right)^m\left(\frac{k_BT_K+\Delta}{D+\Delta}\right)^M, \qquad (2)$$

where T_K is the Kondo temperature, defined for a given Δ by the initial conditions $J=J_0$, $D=D_0$, and $\rho_0=1/(2D_0)$. The relationship between T_K and $J_0(D_0)$ defined by Eq. (2) is sufficient for a qualitative description of the correlation functions in a restricted temperature range (say, between 300 K and 1 K) but is not accurate enough for a quantitative analysis of the low-energy properties in terms of the bare model parameters.

The scaling theory can be used to renormalize the perturbation expansion for the thermopower. First, we reduce the conduction-electron half-bandwidth from D_0 to $D=k_BT$ and find the effective couplings $J(T)$. Next, we notice that the reduction of the bandwidth does not change the form of the Hamiltonian and that the form of the response functions obtained by the perturbation expansion in terms of the effective coupling constants remains invariant with respect to scaling. Thus, to find the thermopower by the RPT we substitute $J(T)$ as given by Eq. (2), with $D=k_BT$, in the BC expressions. Other transport and thermodynamic quantities are found in an analogous way.[75] Strictly speaking, we have different scaling laws above Δ, where the f state is $(m+M)$-fold degenerate, and below Δ, where it is only *m*-fold degenerate, but Eq. (2) seems to provide a reasonable description of the coupling constant renormalization in the LM regime. The range of validity of the RPT is defined by the condition $\rho_0|J(T)|<1$; i.e., an expansion in terms of the renormalized $J(T)$ will break down for temperatures sufficiently close to T_K. The RPT based on somewhat different scaling laws or a different choice of the cutoff procedure gives somewhat different TEP curves but the qualitative features remain the same. Note that the CF splitting reduces the effective degeneracy of the f states, which leads [see Eq. (2)] to an exponential reduction of T_K and extends the range of validity of the perturbation theory to lower temperatures.

The thermopower for the doublet-quartet CF scheme ($m=2$, $M=4$) is given by the expression[50]

$$S=\frac{k_B}{|e|}\frac{S_\Delta}{R_\Delta}G_1(\Delta,0), \qquad (3)$$

where S_Δ and R_Δ are dimensionless quantities given by BC as

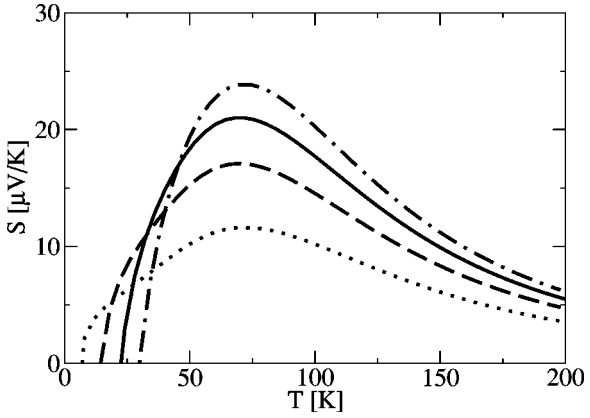

FIG. 2. The thermopower plotted as a function of temperature for $\rho_0 V_0 = -0.35$, $\Delta = 350$ K, and four different values of T_K: dotted curve, $T_K = 2$ K; dashed curve, $T_K = 5$ K; solid curve, $T_K = 8$ K; dot-dashed curve, $T_K = 11$ K.

$$S_\Delta = 16(\rho_0 J)^2 \Bigg[(2\langle n_m\rangle \rho_0 J + 4\langle n_M\rangle \rho_0 J)\tanh\left(\frac{\Delta}{2k_B T}\right) - \rho_0(\tilde{V}_m + J\langle n_m\rangle + \tilde{V}_M + J\langle n_M\rangle)(\langle n_m\rangle - \langle n_M\rangle)\Bigg] \tag{4}$$

and

$$R_\Delta = 2\rho_0^2\left[\tilde{V}_m^2 + 2J^2\langle n_m\rangle\left(1 - \frac{\langle n_m\rangle}{2}\right)\right] + 4\rho_0^2\left[\tilde{V}_M^2 + 4J^2\langle n_M\rangle \times\left(1 - \frac{\langle n_M\rangle}{4}\right)\right] + 16(\rho_0 J)^2\left(\frac{\langle n_m\rangle}{1+e^{\Delta/k_B T}} + \frac{\langle n_M\rangle}{1+e^{-\Delta/k_B T}}\right). \tag{5}$$

Here

$$G_1(\Delta,0) = \frac{\Delta}{k_B T}\left[1 + \frac{\Delta}{2\pi k_B T}\,\mathrm{Im}\,\psi'\left(i\frac{\Delta}{2\pi k_B T}\right)\right] \tag{6}$$

and $\psi'(x)$ is the derivative of the psi (digamma) function.[77] The occupancy of the CF states is

$$\langle n_m\rangle = \frac{1/2}{1+2e^{-\Delta/k_B T}},\quad \langle n_M\rangle = \frac{(1/2)e^{-\Delta/k_B T}}{1+2e^{-\Delta/k_B T}}, \tag{7}$$

and the effective potential scattering on the CF doublet and quartet is

$$\tilde{V}_m = V_0 - J_0\langle n_m\rangle,\quad \tilde{V}_M = V_0 - J_0\langle n_M\rangle, \tag{8}$$

respectively. The renormalized exchange interaction J is temperature dependent due to the flow towards the strong-coupling fixed point (in the renormalization-group sense), while the effective potential scattering, defined by Eq. (8) in terms of V_0 and J_0, is temperature dependent due to the thermal occupation of CF levels.

The thermoelectric power obtained for $D_0 = 1$ eV and for several values of Δ, T_K, and V_0 is shown in Figs. 2–4. The

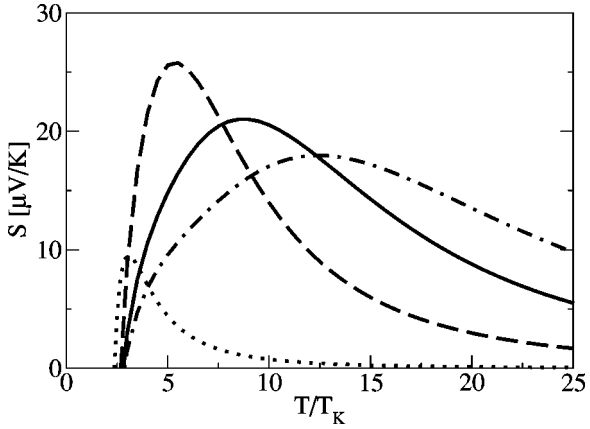

FIG. 3. The thermopower plotted as a function of reduced temperature T/T_K for $T_K = 8$ K, $\rho_0 V_0 = -0.35$, and four values of CF splitting: dotted curve, $\Delta = 50$ K; dashed curve, $\Delta = 200$ K; solid curve, $\Delta = 350$ K; dot-dashed curve, $\Delta = 500$ K.

effect of T_K on $S(T)$ is shown in Fig. 2 for $\Delta = 350$ K and $\rho_0 V_0 = -0.35$. For this negative V_0 and relatively large value of $\rho_0|V_0|$, the high-temperature thermopower is positive and, like in the BC theory, $S(T)$ attains the maximum value at T_{max} which is a fraction of Δ. The value of T_{max} is about the same for all the curves, but $S(T)$ at T_{max} is bigger for larger T_K. We also see a novel feature with respect to the unrenormalized BC expansion. The thermopower obtained by the RPT changes sign at low enough temperatures and the value of the crossing temperature T_x correlates clearly with T_K.

The effect of Δ on $S(T)$ is shown in Fig. 3 for $T_K = 8$ K and $\rho_0 V_0 = -0.35$ on a reduced temperature scale T/T_K. An increase of Δ shifts T_{max}/T_K to higher values but the relationship does not seem to be a simple one. The value of T_x, obtained here for fixed values of V_0 and T_K, is almost independent of Δ. However, Eq. (2) shows that for fixed values of J_0 and D_0, the T_K itself is reduced when Δ increases.

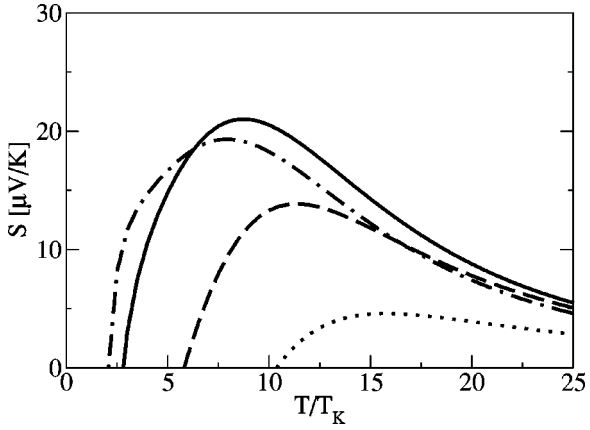

FIG. 4. The thermopower plotted as a function of reduced temperature T/T_K, for $\rho_0 J_0 = -0.035$, $\Delta = 350$ K (giving $T_K = 8$ K), and four values of potential scattering: dotted curve, $\rho_0 V_0 = -0.15$; dashed curve, $\rho_0 V_0 = -0.20$; solid curve, $\rho_0 V_0 = -0.35$; dot-dashed curve, $\rho_0 V_0 = -0.50$.

The effect of V_0 is shown in Fig. 4, where $S(T)$ obtained for $\Delta=350$ K and $T_K=8$ K is plotted on the reduced temperature scale. (Other values of T_K lead to a similar behavior.) For negative V_0 the TEP has a positive maximum which becomes smaller and moves to higher temperatures as V_0 approaches zero. For small enough $\rho_0|V_0|$ the TEP develops a negative peak and for $\rho_0 V_0 \geqslant 0$ this negative peak becomes very large (not shown here). Note that for small $|V_0|$ we have $T_x \gg T_K$; i.e., the TEP changes sign at temperatures where the third-order RPT is still valid. For large enough $|V_0|$, however, a large value of $|J(T)|$ would be needed to reverse the sign of $S(T)$ and T_x would have to approach T_K, so that the sign change cannot take place within the region of validity of the RPT.

The qualitative features of the thermopower described by Eq. (3) and shown in Figs. 2–4 follow straightforwardly from the asymptotic expansion of the elementary functions in Eqs. (3)–(6) and can be summarized as follows. At high temperatures, where $\rho_0 J(T)$ is a slowly varying function, $S(T)$ reduces to the BC expression,[50] and we find a huge TEP maximum which is typical of the LM regime. At low temperatures a new feature emerges: for $k_B T \ll \Delta$, where $\langle n_m \rangle \simeq \frac{1}{2}$ and $\langle n_M \rangle \simeq 0$, Eqs. (4) and (8) give approximately $S_\Delta \propto [J(T) - \frac{4}{3}(V_0 - \frac{1}{4}J_0)]$. Thus, the TEP can change as temperature approaches T_K and, for the ground-state doublet, T_x is given by the solution of $J(T) - \frac{4}{3}V_0 = 0$.

The RPT breaks down for temperatures close to T_K, where $|J(T)|$ is too large for the higher-order terms in the expansion to be neglected. For large values of $\rho_0|V_0|$, this occurs at $T > T_x$ but for small $\rho_0|V_0|$ the RPT remains valid much below T_x, where $S(T)$ is negative. Since $S(T)$ must vanish at $T=0$, the result $S(T_x)=0$ hints at an additional low-temperature minimum or maximum. These low-temperature features, however, have to be calculated by the methods which are appropriate for the strong-coupling limit.

IV. LOW-TEMPERATURE THEORETICAL MODEL

The ground state of the CSM is a Fermi liquid with the local moment screened by the conduction states, and direct calculations of low-temperature thermoelectric properties are difficult. However, for large CF splitting the thermopower can be obtained in a simpler way, because the scattering of conduction electrons on the excited CF states becomes negligibly small and the f moment behaves as an effective doublet with the Kondo scale T_K. Thus, for $T \leqslant T_K$, the CS model can be approximated by a spin-$\frac{1}{2}$ Kondo model, provided the anisotropy of the actual spin-orbit state is neglected. The low-energy properties of such a Kondo model coincide with the properties of a spin-$\frac{1}{2}$ Anderson model with large f-f correlation. Thus, the properties of Ce or Yb systems below T_K can be described by the SIAM in which the f ions fluctuate between zero- and one-electron configurations or between zero- and one-hole configurations, respectively. The equivalence of the two models is easily established by the SW transformation.

The Kondo limit of the SIAM is characterized by a single energy scale, and if one chooses this scale to coincide with the Kondo temperature T_K of the full CSM, the low-temperature properties of the CSM can be obtained from the Hamiltonian

$$H_A = \sum_{l,\sigma} \epsilon_f a^\dagger_{l\sigma} a_{l\sigma} + \sum_{\mathbf{k},\sigma} \epsilon_{\mathbf{k}} c^\dagger_{\mathbf{k}\sigma} c_{\mathbf{k}\sigma} + \sum_{\mathbf{k},l,\sigma} \left(\frac{V_{\mathbf{k}}}{\sqrt{N}} c^\dagger_{\mathbf{k}\sigma} a_{l\sigma} + \text{H.c.} \right) + U \sum_l a^\dagger_{l\uparrow} a_{l\uparrow} a^\dagger_{l\downarrow} a_{l\downarrow}, \tag{9}$$

where l labels the random impurity sites, σ labels the spin states, ϵ_f is the "unrenormalized" ("bare") position of the effective CF ground state, $V_{\mathbf{k}}$ is the hybridization matrix element, and U is the f-f on-site Coulomb repulsion. We consider a conduction band with a semielliptical density of states $\rho_c(\epsilon)$ of half-width W and perform the calculations for $n_c(T)$ conduction electrons per site and the concentration c_i of impurity ions, occupied by $n_f(T)$ f electrons per impurity site. The chemical potential μ is adjusted so as to conserve the total number of particles, $n_{tot} = n_c(T) + c_i n_f(T) = \text{const}$; $n_c(T)$ and $n_f(T)$ are temperature dependent. The hybridization between conduction electrons and f electrons is described by the complex function

$$\Gamma(z) = \frac{1}{N} \sum_{\mathbf{k}} \frac{|V_{\mathbf{k}}|^2}{z - (\epsilon_{\mathbf{k}} - \mu)}, \tag{10}$$

which is the $U=0$ self-energy of f electrons due to hybridization. If $V_{\mathbf{k}}$ is of the form $V_{\mathbf{k}} = V(\epsilon_{\mathbf{k}})$, as is usually assumed, $\Gamma(z)$ can be written in terms of the (unperturbed) conduction-electron density of states as

$$\Gamma(z) = \int_{-\infty}^{\infty} d\epsilon \frac{|V(\epsilon)|^2 \rho_c(\epsilon)}{z - (\epsilon - \mu)}. \tag{11}$$

Close to half-filling, the properties of the model depend on the parameter $u = U/\pi\Gamma$, where $\Gamma = \pi|V|^2/(2W)$ is the relevant energy scale for localized electrons in the absence of U. Since the doubly occupied f states should be excluded, the thermoelectric properties have to be calculated for large values of u.

The TEP of the SIAM is given by the expression[48]

$$S = \frac{k_B}{|e|T} \frac{\int dE \left(-\frac{df}{dE} \right) (E-\mu) L(E)}{\int dE \left(-\frac{df}{dE} \right) L(E)}, \tag{12}$$

where $f(E) = (e^{E/k_B T} + 1)^{-1}$ is the Fermi function, $L(E)$ is the static limit of the frequency-dependent conductivity, here given by

$$\frac{1}{L(\omega)} = \mp \frac{2\Gamma}{\pi} \text{Im}\, G_f(\omega \pm i0^+), \tag{13}$$

and $G_f(z)$ is the f-electron Green's function defined by the Dyson equation

$$G_f(z) = \frac{1}{z - (\epsilon_f - \mu) - \Gamma(z) - U n_f/2 - \tilde{\Sigma}(z)}. \tag{14}$$

Here, $n_f = n_{f\uparrow} + n_{f\downarrow}$ is the renormalized number of f electrons,

$$n_f = 2\int_{-\infty}^{\infty} d\omega f(\omega)\left[\mp\frac{1}{\pi}\mathrm{Im}\, G_f(\omega \pm i0^+)\right], \qquad (15)$$

$Un_f/2$ is the frequency-independent part of the f-electron self-energy, and $\tilde{\Sigma}(z)$ is its frequency-dependent part, which has to be calculated for large values of u.

An approximate solution is provided by the MPT expression[70] which interpolates between the second-order weak-coupling self-energy and its exact atomic limit, and which reads

$$\tilde{\Sigma}(z) = \frac{\Sigma^{(2)}(z)}{1 - \dfrac{(1-n_f/2)U + (\epsilon_l - \epsilon_0)}{(n_f/2)(1-n_f/2)U^2}\Sigma^{(2)}(z)}. \qquad (16)$$

$\Sigma^{(2)}(z)$ is the analytic continuation of the second-order self-energy diagram,

$$\Sigma^{(2)}(i\omega_n) = -U^2 k_B T \sum_{\nu_k} G_f^{(0)}(i\omega_n + i\nu_k) k_B T \sum_{\omega_m} G_f^{(0)}(i\omega_m) G_f^{(0)}(i\omega_m + i\nu_k), \qquad (17)$$

calculated on the imaginary axis with auxiliary $U=0$ unperturbed Green's functions

$$G_f^{(0)}(z) = \frac{1}{z - (\epsilon_0 - \mu) - \Gamma(z)}, \qquad (18)$$

where $\omega_n = (2n+1)\pi k_B T$ and $\nu_n = 2n\pi k_B T$. The number of particles in this auxiliary "virtual bound state" is

$$n_f^0 = 2\int_{-\infty}^{\infty} d\omega f(\omega)\left[\mp\frac{1}{\pi}\mathrm{Im}\, G_f^{(0)}(\omega \pm i0^+)\right], \qquad (19)$$

and ϵ_0 is determined by the condition $n_f^0 = n_f$.

The f-electron spectral function obtained by the MPT is plotted in Fig. 5 as a function of frequency for several temperatures. The calculations are performed for $\Gamma = 0.045W$, $U = 0.5W$ ($u = 3.537$), and $n_{tot} = 0.88$, $c_i = 0.1$ (which means a 10% alloy), and $n_f(0) = 0.8$ (so that the conduction band is close to half filling.) The ground state of this system is characterized by an asymmetric Kondo resonance in $\rho_f(\omega)$, centered slightly above the chemical potential ($\omega = 0$); i.e., the system is in the strong-coupling limit. The half-width of this resonance defines T_K, and for the data shown in Fig. 5 we find $k_B T_K = 0.0175W$. Note that almost the same value of T_K is defined by the temperature at which $\rho_f(\omega = 0)$ drops to one half of its zero-temperature value. The spectral properties obtained by the MPT show all the expected strong-coupling features. In particular, the Kondo resonance becomes smaller at higher temperatures and above T_K it merges with the occupied single-particle states. The f-electron occupation is also temperature dependent and it

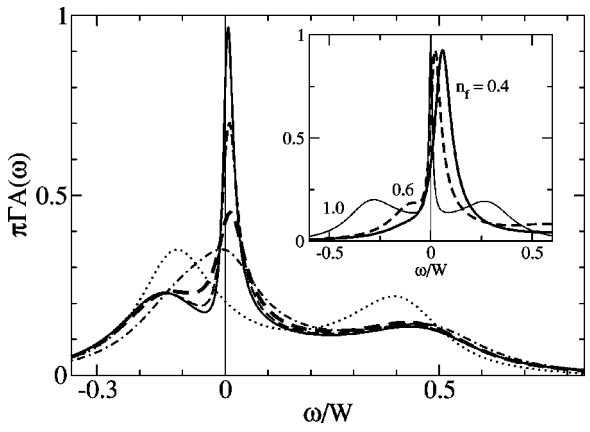

FIG. 5. The f-electron spectral function for the SIAM with an elliptical density of states, plotted as a function of frequency, for $\Gamma = 0.045W$, $U = 0.5W$, $n_{tot} = 0.88$, and $c_i = 0.1$, giving $k_B T_K = 0.0175W$, at $T = 0.03T_K$ (solid line), $0.5T_K$, T_K, $2T_K$, and $10T_K$ (dotted line). The inset shows the evolution of the spectral function at $T = 5\times10^{-4}W$ towards the empty orbital regime (n_f indicated in the figure, other parameters the same as above).

grows from $n_f(0) = 0.8$ at $T = 0$ to about $n_f = 0.85$ at T_K. The Kondo resonance obtained for other concentrations of f ions and other values of n_f behaves in a similar way; for a given value of n_{tot}, the lowest T_K is obtained for $n_f = 1$. However, if n_f is reduced below some value [$n_f(0) = 0.6$ for the parameters used in Fig. 5], the Kondo resonance merges with the left single-particle peak ("wing"), and the system is a valence fluctuator (see the inset in Fig. 5).

As regards the thermopower, we notice first that it vanishes for systems with electron-hole symmetry ($n_f = n_c = 1$) and that it remains very small for $n_f = 1$ and $n_c \approx 1$. Close to the ground state we find a linear temperature dependence

$$\lim_{T\to 0} S(T) = \frac{\pi^2 k_B}{3|e|}\cot\left(\frac{\pi}{2}n_f\right)\frac{T}{T_K}, \qquad (20)$$

where $(\pi/2)n_f = \eta_0(\epsilon_F)$, the resonant phase shift due to the scattering of conduction electrons on the f state. The initial growth of the TEP is very fast ($\pi^2 k_B/3|e| = 284\ \mu V/K$) and the initial sign coincides with the slope of $\rho_f(\omega)$ at $\omega = 0$. The shape of $S(T)$ at higher temperatures is determined by the nonlinear correction, but as long as the system is in the Fermi-liquid regime we expect a universal power-law behavior $S(T) \propto (T/T_K)[1 - B(n_f)(T/T_K)^2]$, where the coefficient $B(n_f)$ can be obtained from Eq. (12) by the Sommerfeld expansion. The sign of the TEP follows the slope of $\rho_f(0)$ even at elevated temperatures and Fig. 5 indicates, for Kondo ions with $n_f \simeq 1$, a sign change at about $T \simeq T_K$.

The temperature dependence of the thermopower calculated for the same Γ, U, c_i, and n_{tot} as in Fig. 5 is shown in Figs. 6 and 7 as a function of T/T_K, for various values of $n_f(0)$. All curves in Figs. 6 and 7 have the initial (low-T) slopes given by Eq. (20). The $n_f(0) = 1$ result (not shown in either Fig. 6 or Fig. 7) is negligibly small, because $\rho_c(\epsilon)$ is very flat around μ for $n_c(0) = 0.8$ and $\rho_f(\omega)$ is almost symmetric. We also note that the absolute value of the TEP at the maximum or minimum increases as either $n_f(0)$ or $n_f^{hole}(0)$

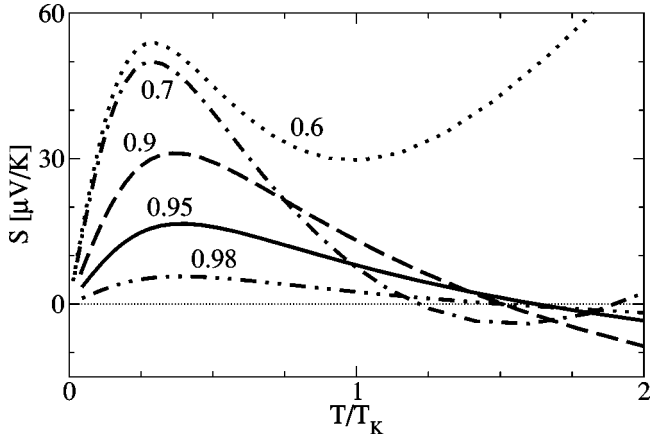

FIG. 6. The thermopower of the SIAM as a function of temperature, measured in units of T_K, shown for various numbers of f electrons (indicated in the figure) and for the same values of other parameters as in Fig 5. The corresponding values of T_K are $k_B T_K/W=0.011$ [for $n_f(0)=0.98$], 0.011, 0.012, 0.025, and 0.035 [for $n_f(0)=0.6$], respectively.

is decreased below 0.98. That is, systems with large T_K have large TEP. The highest values are found for the valence-fluctuation systems. A very small T_K, on the other hand, leads to only a small TEP in the FL regime. All the MPT curves shown here are obtained for $c_i=0.1$—i.e., for a 10% alloy—but the same qualitative features are found for other concentrations, including $c_i=1$.

The curves in Fig. 6 give the TEP due to an ion which fluctuates between the $4f^0$ and $4f^1$ configurations. Those obtained for $0.98\geqslant n_f(0)\geqslant 0.6$ show a positive initial slope, a maximum around $T_K/2$ and a change of sign between T_K and $2T_K$. However, for $n_f=0.7$ the negative values of $S(T)$ are very small and restricted to a narrow temperature range. Further reduction of n_f leads to the TEP which does not change sign above the low-temperature peak, but still exhibits a nonmonotonic behavior, as shown by the curve for $n_f=0.6$. Finally, for $n_f\leqslant 1$ the Kondo resonance does not appear at all and the TEP increases monotonously from zero.

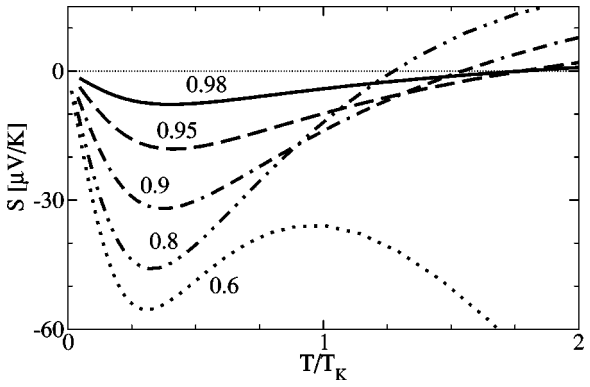

FIG. 7. The thermopower of the SIAM as a function of temperature, measured in units of T_K, shown for various numbers of f holes (indicated in the figure). The corresponding values of T_K are $k_B T_K=0.011$ [for $n_f^{hole}(0)=0.95$], 0.013, 0.018, and 0.035 [for $n_f^{hole}(0)=0.6$], respectively.

The curves in Fig. 7 give the TEP due to an ion which fluctuates between the full f shell and the one-f-hole configuration; this corresponds to Yb ions. Figure 7 is *not* a perfect "mirror image" of Fig. 6, since the system is not electron-hole symmetric due to $n_c(0)\neq 1$. The $S(T)$ curves obtained for $0.98\geqslant n_f^{hole}(0)\geqslant 0.8$ show a negative initial slope, a minimum around $T_K/2$, and a change of sign between T_K and $2T_K$. Further reduction of $n_f^{hole}(0)$ leads to the TEP which does not change sign at all, but still shows a nonmonotonic behavior [see the curve corresponding to $n_f^{hole}(0)=0.6$].

Finally, we comment on the validity of the MPT calculations. We notice, first, that the zero-temperature MPT results for the renormalized f-particle number and the charge susceptibility agree with the Bethe ansatz solution, even for very large values of u.[70] The temperature dependence of the Kondo resonance, calculated for $u>1$, agrees very well with the numerical renormalization group (NRG) results,[56,57] and the Fermi-liquid laws given by the MPT are also nearly the same.[56,57] Thus, we believe that the TEP obtained by the MPT is qualitatively correct even in the strong-coupling limit, which is needed for the description of Ce and Yb systems. The reason for the successful application of the perturbation theory is that the strong-coupling behavior of the SIAM sets in as soon as $u\geqslant 2$, and the perturbational results for the coefficients in the power-law expansion of the correlation functions (in terms of T/T_K) are not too far off of the universal FL values. Clearly, the MPT cannot provide a correct expression for T_K in terms of the parameters of the model; this requires exact calculations. But the shape of the thermopower obtained in the FL regime by the MPT, plotted on the universal T/T_K scale, should not be much different from the exact result. On the other hand, the MPT is not expected to be accurate above T_K, since an expansion above the noninteracting FL ground state is not a very good starting point for describing the LM regime. However, we are not concerned here with the high-temperature properties of an m-fold degenerate model which neglects the excited CF states.

V. DISCUSSION OF THE THEORETICAL RESULTS AND CONCLUSION

The experimental data presented in Sec. II have many features in common with the low- and high-temperature results discussed in Secs. III and IV. In what follows we compare theory and experiment assuming $n_f\leqslant 1$, which is appropriate for cerium ions; the results pertaining to ytterbium ions ($n_f^{hole}\leqslant 1$) can be obtained by reflecting the cerium curves on the temperature axis.

At high temperatures $k_B T_K<k_B T\ll\Delta$, the thermopower is calculated by the RPT, and we recall that the exchange and potential scattering, generated by the SW transformation, have the same sign for Ce ions but the opposite sign for Yb ions. Thus, we obtain the TEP of Ce systems with a large positive peak centered at a temperature T_{max}, which is typically a fraction of Δ/k_B. This peak is asymmetric and much steeper on the low- than on the high-temperature side, as often seen in cerium systems above 100 K. The position of T_{max} depends not only on T_K and Δ, but on the strength of

the effective potential scattering as well, which should be kept in mind when comparing the theory with the experimental data. The RPT also shows that $S(T)$ changes sign at $T_x \simeq \alpha T_K$, where $\alpha \simeq 1$ for large potential scattering and $\alpha \gg 1$ in the opposite case. For the values of model parameters used in this paper we found $2.5 \leqslant \alpha \leqslant 10$; i.e., for $\rho_0|V_0| \leqslant 0.2$ a negative TEP is obtained well within the range of validity of the RPT. The sign change at T_x and the ensuing negative TEP of Ce ions are an important improvement with respect to the earlier calculations based on an unrenormalized perturbation expansion,[50] which predicted a monotonic decrease of $S(T)$ below T_{max} and hence could not explain the TEP of $CeAl_3$ and many other Ce compounds. The sign change obtained here is due to the renormalization of the exchange constant and is an indication of the onset of the strong-coupling behavior. For the doublet-quartet CF scheme this occurs for $|J(T)| \geqslant \frac{4}{3}|V_0|$. We notice also that the values of the exchange and potential scattering should be smaller for Ce ions with one f electron than for Ce ions with a reduced f count. Thus, the systems which have $n_f \simeq 1$, low T_K, and small $\rho_0|V_0|$ acquire a negative TEP much above T_K, while in systems with significant potential scattering ($n_f < 1$) the sign change does not occur at temperatures at which the RPT is valid. This is consistent with the experimental data, which show negative TEP for Ce ions in a stable magnetic configuration and with small T_K (experimentally, T_x is between several K and roughly 100 K, and $T_x \gg T_K$) and the absence of the negative TEP for Ce ions with large T_K or in the valence-fluctuating systems.

At low temperatures $k_B T \leqslant k_B T_K \ll \Delta$, the excited CF states can be neglected and for the doublet-quartet scheme the CSM becomes equivalent to an effective spin-$\frac{1}{2}$ Anderson model. For Ce ions we require $n_f \leqslant 1$; i.e., the effective low-temperature model is not too far off of the electron-hole symmetry. The FL properties of such a model are very well described by the MPT, even for a large coupling, and we find that the TEP has an initial linear rise $S(T) \propto T/T_K$, after which it saturates and attains a positive maximum at about $T_K/2$. For cerium Kondo ions, the TEP becomes negative above T_K. The size of the TEP maximum and the temperature of the sign change increase as n_f is reduced from 1 and for $n_f < 0.7$ the TEP is large and always positive. On the other hand, for $n_f \simeq 1$ the positive values reached by the TEP are very small, as shown by Fig. 6. These results agree with recent measurements[43,44,47] which show that the slope $S(T)/T$ is positive for most Ce heavy fermions if the measurements are performed at low enough temperature and with sufficient accuracy. The TEP of Yb ions in the FL regime is obtained from a SIAM with $n_f^{holes} \leqslant 1$. We find a similar pattern as for Ce ions but with the reversed sign.

If we use the same Kondo temperature in the LM and FL regimes, and plot $S(T)$ on a universal T/T_K scale, we can combine the LM data shown in Figs. 3 and 4 with the FL data in Figs. 6 and 7, and estimate the overall shape of $S(T)$. The quantitative analysis is difficult, however, because there are additional parameters, besides T_K, which influence the RPT and MPT results. On a qualitative level, we find that the thermopower of the CSM exhibits all the typical shapes[35,36] discussed in Sec. II. For Ce ions with a large CF splitting and $n_f \simeq 1$—i.e., for systems with small T_K and small potential scattering—we obtain the TEP with a positive maximum at high temperature, which is due to the scattering on the full f multiplet, and a broad temperature interval in which the TEP is negative. Since T_K is very small, the positive bump predicted by the MPT in the FL regime is experimentally irrelevant, and the overall shape of the TEP is of the (a) type. For higher values of T_K (obtained for $n_f \leqslant 1$ and/or smaller values of u) the positive low-temperature maximum becomes visible and the TEP exhibits two positive peaks separated by a negative minimum; i.e., TEP of type (b) is found. In this part of the parameter space, the separation between the two positive peaks is still large but the temperature interval in which the TEP is negative is smaller than in type (a) systems. We also remark that most type (a) and many type (b) systems order magnetically at low temperatures, but in our calculations the negative low-temperature TEP is related to the crossover from the LM regime to the FL regime; i.e., it is due to the single-ion Kondo effect and not to the magnetic interaction between Ce ions, which is neglected. The type (c) behavior is obtained for the CSM with large CF splitting and $n_f < 1$, such that $S(T)$ has a large FL maximum and no sign change above T_K, as seen in Fig. 6 for $n_f = 0.6$. These FL results should be combined with the high-temperature results obtained by the RPT for large potential scattering, i.e., with the TEP which is positive for $T \geqslant T_K$, as shown in Fig. 4 for $\rho_0|V_0| \geqslant 0.5$. The overall separation between the FL and LM peaks is now reduced and the crossover from the high-temperature LM regime to the low-temperature FL regime occurs without a sign change of $S(T)$. This crossover is indicated just by a shallow minimum or a shoulder on the low-temperature side of the LM peak. Type (c) or (d) behavior can also arise if the CF splitting is reduced sufficiently, which makes the characteristic temperature so large that $S(T)$ increases monotonically up to room temperature.

The overall temperature dependence of the TEP in ytterbium systems is equally well explained by the CSM model with CF splitting. A good example is provided by $YbNi_2Si_2$ (Ref. 39) or $Yb_2Rh_3Al_9$ (Ref. 40), which show a large negative high-temperature peak of the TEP due to the exchange scattering on the CF-split f multiplet and a negative FL peak due to the scattering on the ground-state doublet or quartet. The negative LM peak of Yb systems is often found at lower temperatures than in Ce systems and is usually centered below 100 K.

The CSM model explains also the variation of the TEP due to pressure or chemical pressure. To discuss these effects we assume that pressure increases the hybridization and/or shifts the f level with respect to the chemical potential, which enhances T_K and reduces n_f of a given Ce ion. We also assume that the potential scattering of the CSM, generated by the SW transformation from an underlaying SIAM, is enhanced with respect to the zero-pressure values. We then find the renormalized exchange coupling $J(T)$, corresponding to the enhanced T_K, and calculate the TEP in the LM regime using the RPT.[78] This leads to $S(T)$ which has the maximum at higher temperatures and the sign change at lower temperatures, than at zero pressure. In the FL regime

the MPT calculations[79] for the same T_K—i.e., for reduced n_f—give the TEP which has an enhanced FL maximum and has the onset of negative TEP shifted to higher temperature (on an absolute scale). For small enough n_f, the sign change is absent altogether and the TEP is always positive. Putting these calculations together we find, for Ce Kondo ions, that pressure enhances the low- and high-temperature TEP peaks with respect to the zero-pressure values, shifts both peaks to higher temperatures, and reduces the peak-to-peak separation. Thus, the CSM explains the emergence of a small positive peak and the reduction of the temperature interval in which the TEP is negative, which is often observed at moderate pressure in Ce systems with large CF splitting and small T_K. At higher pressure the exchange and potential scattering should be further increased, such that the TEP does not become negative in the LM regime. Since n_f is also reduced, the FL thermopower is always positive, and the crossover between the two regimes proceeds without a sign change. The TEP exhibits now a two-peak structure but is never negative. Eventually, at very high pressure, the two peaks merge, and a complete change from type (a) or (b) to (c) and (d) occurs. This explains the evolution of the TEP found in pressure experiments on $CeCu_2Si_2$ (Ref. 13) and several other systems discussed in Sec. II. It also explains the doping dependence, if we assume that doping with smaller ions enhances hybridization and doping with larger ions has the opposite effect. The corresponding behavior of ytterbium systems, like YbSi (Ref. 42) or $YbNi_2Si_2$ (Ref. 39), follows along the same lines, provided we take into account that pressure increases the hybridization and brings the number of f holes closer to 1, which stabilizes the magnetic $4f^{13}$ configuration and reduces T_K.

In summary, the overall behavior of the thermoelectric power of the Coqblin-Schrieffer model, with the crystal-field-split f states, agrees with the experimental data on Ce and Yb systems described in Sec. II. The model relates the temperature, pressure, and doping dependence of the thermopower of cerium and ytterbium systems to an interplay between the exchange scattering, potential scattering, and CF splitting. The seemingly complicated shape of $S(T)$ is due to the Kondo effect which leads to a crossover between the weak-coupling LM regime at high temperatures and the strong-coupling FL regime at low temperatures. The quantitative comparison, however, is difficult, because neither the RPT which we use in the LM regime nor the MPT which we use in the FL regime can locate the position of the negative minimum or give a reliable estimate of the TEP at the minimum. Our results give a qualitative explanation of the TEP of dilute alloys and of stoichiometric compounds, despite the fact that the CSM model does not describe correctly the ground state of a Kondo lattice. One way to understand such a good description of ordered compounds by the CSM is to express the thermopower in terms of the reversible Peltier heat and relate it to the entropy of the electron gas. It seems that most of the entropy is removed by local screening of the f moment by the single-ion Kondo effect and that quantum coherence, which sets in at low temperatures and is most important for electrical resistivity, gives rise to additional terms which do not change the entropy or thermopower in a qualitative way. However, a proper treatment of the low-temperature thermoelectric properties of ordered compounds requires a lattice model, and these calculations are the subject of our future work.

ACKNOWLEDGMENT

We acknowledge useful comments from I. Aviani, A. K. Bhattacharjee, J. Freericks, A. Hewson, M. Očko, C. Geibel, J. R. Iglesias, R. Monnier, and F. Steglich. One of us (V.Z.) gratefully acknowledges financial support from the Humboldt Foundation and the Swiss NSF (Project No. 7KRPJ065554-01/1). We also thank the French-Croatian Cooperation (MS&T, Croatia and CNRS, France) for financial support.

*Electronic address: zlatic@ifs.hr

[1] P.B. van Aken, H.J. van Daal, and K.H.J. Buschow, Phys. Lett. **49A**, 201 (1974).
[2] H.J. van Daal, P.B. van Aken, and K.H.J. Buschow, Phys. Lett. **49A**, 246 (1974).
[3] F. Steglich, Festkoerperprobleme **17**, 319 (1977).
[4] T.S. Petersen, S. Legvold, J.O. Moorman, O.D. McMasters, and K.A. Gschneider, Jr., J. Appl. Phys. **50**, 6363 (1979).
[5] E.M. Levin, R.V. Lutsiv, L.D. Finkel'shteĭn, N.D. Samsonova, and R.I. Yasnitskiĭ, Sov. Phys. Solid State **23**, 1403 (1981).
[6] H. Schneider, Z. Kletowski, F. Oster, and D. Wohlleben, Solid State Commun. **48**, 1093 (1983).
[7] F.G. Aliev, N.B. Brandt, V.V. Moshchalkov, O.V. Petrenko, and R.I. Yasnitskiĭ, Sov. Phys. Solid State **26**, 682 (1984).
[8] G. Sparn, W. Lieka, U. Gottwick, F. Steglich, and N. Grewe, J. Magn. Magn. Mater. **47&48**, 521 (1985).
[9] U. Gottwick, K. Gloos, S. Horn, F. Steglich, and N. Grewe, J. Magn. Magn. Mater. **47&48**, 536 (1985).
[10] J. Sakurai, T. Ohyama, and Y. Komura, J. Magn. Magn. Mater. **47&48**, 320 (1985).
[11] J. Sakurai, H. Kamimura, and Y. Komura, J. Magn. Magn. Mater. **76&77**, 287 (1988).
[12] A. Amato and J. Sierro, J. Magn. Magn. Mater. **47&48**, 526 (1985).
[13] D. Jaccard, J.M. Mignot, B. Bellarbi, A. Benoit, H.F. Braun, and J. Sierro, J. Magn. Magn. Mater. **47&48**, 23 (1985).
[14] D. Jaccard and J. Flouquet, Helv. Phys. Acta. **60**, 108 (1987).
[15] U. Gottwick, R. Held, G. Sparn, F. Steglich, K. Vey, W. Assmus, H. Rietschel, G.R. Stewart, and A.L. Giorgi, J. Magn. Magn. Mater. **63&64**, 342 (1987).
[16] D. Jaccard, M.J. Besnus, and J.P. Kappler, J. Magn. Magn. Mater. **63&64**, 572 (1987).
[17] Y. Onuki and T. Komatsubara, J. Magn. Magn. Mater. **63&64**, 281 (1987).
[18] J. Sakurai, T. Ohyama, and Y. Komura, J. Magn. Magn. Mater. **63&64**, 578 (1987).
[19] A. Amato, Ph.D. thesis, University of Geneve, Geneve, 1988.
[20] A. Amato, D. Jaccard, J. Sierro, F. Lapierre, P. Haen, P. Lejay, and J. Flouquet, J. Magn. Magn. Mater. **76&77**, 263 (1988).
[21] C. Fierz, D. Jaccard, and J. Sierro, J. Appl. Phys. **63**, 3899 (1988).

[22] E. Gratz, E. Bauer, R. Hauser, N. Pillmayr, G. Hilscher, H. Müller, and B. Barbara, J. Magn. Magn. Mater. **76&77**, 275 (1988).
[23] J. Sakurai, H. Kamimura, and Y. Komura, J. Magn. Magn. Mater. **76&77**, 287 (1988).
[24] E.V. Sampathkumaran, R. Vijayaraghavan, A. Adam, Y. Yamamoto, Y. Yamaguchi, and J. Sakurai, Solid State Commun. **71**, 71 (1989).
[25] Y. Yamaguchi, J. Sakurai, F. Teshima, H. Kawanaka, T. Takabatake, and H. Fuji, J. Phys.: Condens. Matter **2**, 5715 (1990).
[26] M.R. Lees, B.R. Coles, E. Bauer, and N. Pillmayr, J. Phys.: Condens. Matter **2**, 6403 (1990).
[27] R. Casanova, D. Jaccard, C. Marcenat, N. Hamdaoui, and M.J. Besnus, J. Magn. Magn. Mater. **90&91**, 587 (1990).
[28] D. Jaccard, A. Basset, J. Sierro, and J. Pierre, J. Low Temp. Phys. **80**, 285 (1990).
[29] J. Sakurai, Y. Yamaguchi, K. Mibu, and T. Shinjo, J. Magn. Magn. Mater. **84**, 157 (1990).
[30] E. Bauer, Adv. Phys. **40**, 417 (1991).
[31] R. Cibin, D. Jaccard, and J. Sierro, J. Magn. Magn. Mater. **108**, 107 (1992).
[32] D. Jaccard, K. Behnia, and J. Sierro, Phys. Lett. A **163**, 475 (1992).
[33] Y. Bando, J. Sakurai, and E.V. Sampathkumaran, Physica B **186-188**, 525 (1993).
[34] J. Sakurai, J.C. Gomez Sal, and J. Rodriguez Fernandez, J. Magn. Magn. Mater. **140-144**, 1223 (1995).
[35] J. Sakurai, H. Takagi, S. Taniguchi, T. Kuwal, Y. Isikawa, and J.-L. Tholance, J. Phys. Soc. Jpn. **65**, Suppl. B #49 (1996).
[36] P. Link, D. Jaccard, and P. Lejay, Physica B **225**, 207 (1996).
[37] M. Očko, B. Bushinger, C. Geibel, and F. Steglich, Physica B **259-261**, 87 (1999).
[38] G. Nakamoto, T. Nobata, S. Ueda, Y. Nakajima, T. Fujioka, and M. Kurisu, Physica B **259-261**, 154 (1999).
[39] D. Andreica, K. Alami-Yadri, D. Jaccard, A. Amato, and A. Schenk, Physica B **259-261**, 144 (1999).
[40] O. Trovarelli, C. Geibel, B. Buschinger, R. Borth, S. Mederle, M. Grosche, G. Sparn, and F. Steglich, Phys. Rev. B **60**, 1136 (1999).
[41] O. Trovarelli, C. Geibel, R. Cardoso, S. Mederle, R. Borth, B. Buschinger, F.M. Grosche, Y. Grin, G. Sparn, and F. Steglich, Phys. Rev. B **61**, 9467 (2000).
[42] K. Alami-Yadri, H. Wilhelm, and D. Jaccard, Physica B **259-261**, 157 (1999).
[43] D. Huo, K. Mori, T. Kuwai, S. Fukuda, Y. Isikawa, and J. Sakurai, Physica B **281&282**, 101 (2000).
[44] J. Sakurai, D. Huo, D. Kato, T. Kuwai, Y. Isikawa, and K. Mori, Physica B **281&282**, 98 (2000).
[45] M. Očko, D. Drobac, C. Geibel, and F. Steglich, Phys. Rev. B **64**, 195106 (2001).
[46] M. Očko, C. Geibel, and F. Steglich, Phys. Rev. B **64**, 195107 (2001).
[47] D. Huo, T. Kuwai, T. Mizushima, Y. Isikawa, and J. Sakurai, Physica B **312&313**, 232 (2002).
[48] G. Mahan, B. Sales, and J. Sharp, Phys. Today **50**(3), 42 (1997).
[49] I. Peschel and P. Fulde, Z. Phys. **238**, 99 (1970).
[50] A.K. Bhattacharjee and B. Coqblin, Phys. Rev. B **13**, 3441 (1976).
[51] S. Maekawa, S. Kashiba, M. Tachiki, and S. Takahashi, J. Phys. Soc. Jpn. **55**, 3194 (1986).
[52] N.E. Bickers, D.L. Cox, and J.W. Wilkins, Phys. Rev. B **36**, 2036 (1987).
[53] K. Fischer, Z. Phys. B: Condens. Matter **76**, 315 (1989).
[54] R. Monnier, L. Degiorgi, and B. Delley, Phys. Rev. B **41**, 573 (1990).
[55] S.M.M. Evans, A.K. Bhattacharjee, and B. Coqblin, Phys. Rev. B **45**, 7244 (1992).
[56] V. Zlatić, T.A. Costi, A.C. Hewson, and B.R. Coles, Phys. Rev. B **48**, 16 152 (1993).
[57] T.A. Costi, A.C. Hewson, and V. Zlatić, J. Phys.: Condens. Matter **6**, 2519 (1994).
[58] V. Zlatić and B. Horvatić, J. Phys. F: Met. Phys. **12**, 3075 (1982).
[59] V. Zlatić and N. Rivier, J. Phys. F: Met. Phys. **4**, 732 (1974).
[60] G. Mahan, in *Solid State Physics*, edited by H. Ehrenreich (Academic Press, New York, 1997), Vol. 51, p. 82.
[61] B. Coqblin and J.R. Schrieffer, Phys. Rev. **185**, 847 (1969).
[62] P.W. Anderson, J. Phys. C **3**, 2346 (1970).
[63] P. Nozieres and A. Blandin, J. Phys. (Paris) **41**, 193 (1980).
[64] K. Yamada, K. Yosida, and K. Hanzawa, Prog. Theor. Phys. **71**, 450 (1984); Suppl. Prog. Theor. Phys. **108**, 141 (1992).
[65] K. Hanzawa, K. Yamada, and K. Yosida, J. Magn. Magn. Mater. **47&48**, 357 (1985).
[66] A.C. Hewson, *The Kondo Problem to Heavy Fermions* (Cambridge University Press, Cambridge, United Kingdom, 1993).
[67] J.R. Schrieffer and P.A. Wolff, Phys. Rev. **149**, 491 (1966).
[68] P. Schlottmann, Phys. Rep. **181**, 1 (1998).
[69] B. Cornut and B. Coqblin, Phys. Rev. B **5**, 4541 (1972).
[70] A. Martín Rodero, E. Louis, F. Flores, and C. Tejedor, Phys. Rev. B **33**, 1814 (1986).
[71] K. Yosida and K. Yamada, Prog. Theor. Phys. **53**, 1286 (1975).
[72] V. Zlatić and B. Horvatić, Phys. Rev. B **28**, 6904 (1983).
[73] B. Horvatić and V. Zlatić, J. Phys. (Paris) **46**, 1459 (1985).
[74] For example, an increase of La concentration (negative chemical pressure) in Ce-rich $Ce_xLa_{1-x}Cu_{2.05}Si_2$ alloys (Ref. 45) increases the positive high-temperature peak and reduces the magnitude of the low-temperature negative minimum until, for $x \simeq 0.5$, we obtain the TEP which is always positive and has an additional small peak around 10 K, which is inconsistent with pressure data (Ref. 13).
[75] I. Aviani, M. Miljak, V. Zlatić, K.-D. Schotte, C. Geibel, and F. Steglich, Phys. Rev. B **64**, 184438 (2001).
[76] The magnetic susceptibility of $Ce_xY_{1-x}Cu_2Si_2$ above 100 K is Curie-Weiss like (Ref. 75). It corresponds to a six-fold-degenerate local moment which interacts weakly with the conduction band. Below 20 K the susceptibility corresponds to a two-fold-degenerate local moment with $T_K \leqslant 10$ K. Below 10 K, the susceptibility deviates from the Curie-Weiss form and the local-moment description breaks down.
[77] *Handbook of Mathematical Functions*, edited by M. Abramowittz and I.A. Stegun (Dover, New York, 1965).
[78] The second-order scaling equation (2) is not accurate enough to provide the new value of T_K which would correspond to J_0 changed by pressure. To describe the pressure experiments we treat T_K and V_0 as independent variables.
[79] Here, n_f is varied by changing ϵ_f but similar results are obtained if ϵ_f is kept constant and n_f is changed by varying the hybridization.